SONAR-BASED BURIED OBJECT DETECTION VIA STATISTICS OF RECURRENCE PLOT QUANTIFICATION MEASURES

Joseph Milton, Benjamin Halkon *and* Sebastian Oberst

School of Mechanical and Mechatronic Engineering, University of Technology Sydney, Sydney, Australia.
Centre for Audio, Acoustics and Vibration, University of Technology Sydney, Sydney, Australia.
e-mail: joseph.milton@uts.edu.au

Yan Kei Chiang *and* David Powell

School of Engineering & Information Technology, University of New South Wales, Canberra, Australia.

Active sonar has been successfully deployed for naval mine countermeasures (MCM) to detect, localise, and classify mines and mine-like objects (MLOs). One of the most challenging problems in MCM operations is the detection and classification of (partially) covered objects; traditional image-based sonar processing techniques cannot readily detect objects within the seabed. In this paper, a processing technique that utilises recurrence plot quantification analysis, a class of nonlinear time series analysis, is proposed for improved covered MLO detection in raw sonar signals. Recurrence plots are binary, graphical visualisations of the recurrence matrix generated from time series data. Following an embedding process to reconstruct a copy of the dynamics in phase space, recurrence plot quantification analysis measures can be extracted and further statistically analysed. Using computationally generated sonar signals extracted from simplified representations of real-world relevant scenarios, this study explores the application of such an approach and its sensitivity to the user-defined parameters for detecting the presence of an MLO, irrespective of the level of burial.

Keywords: Underwater acoustics, Recurrence plots, Buried object detection

1. Introduction

Since the early 20th century active sonar-based techniques have been widely used for underwater object detection and localisation, with application across military, commercial and scientific industries [1]. However, with the ever-increasing threat posed by naval mine warfare due to the vast number of unrecovered mines, both historic and present day [2, 3], mine-like-object (MLO) classification is becoming increasingly important, particularly in the cluttered littoral environment. In recent years, numerous sonar scanning and signal processing techniques have been proposed which aim to increase the accuracy of MLO classification [4]. Such techniques often rely on high resolution sonar imagery to visually detect and classify MLOs based on their outer geometry [4, 5]. However, a persistent challenge for these

image-based techniques remains detection and classification of MLOs when embedded within the seabed as the sediment masks identifiable features.

To try to overcome this challenge, previous work has explored the use of lower frequency sonar (2 - 20 kHz) to enhance the detection and classification of buried and partially buried MLOs [6, 7, 8]. Lower frequency sonar is better able to search beneath the sea floor as it can more readily penetrate the sediment [9]. However, due to the longer wavelengths of low frequency sonar, these techniques can struggle to create sufficiently high-resolution sonar images for image-based classification. The lower frequencies are, however, better able to excite strongly scattering structural resonances within man-made structures, including MLOs. This scattering yields information about the dynamics of the MLOs which can be effectively used for object classification, often with reference to a large database of known acoustic scattering responses [10]. Much of the previous work in this area has investigated exploiting the temporal and spectral features of the returning sonar time series to detect and classify MLOs. However, these features do not reveal all of the useful information contained within the time series.

Nonlinear dynamics tools and complexity measures, in particular nonlinear time series analysis (NTSA), could provide insights into the contents of sonar time series that the temporal and spectral methods may miss, especially when contaminated with noise [11]. NTSA studies the dynamics of a system in some multidimensional phase space where all possible states of a system are represented along phase space trajectories [12, 13]. Using this phase space it is possible to quantify certain dynamically invariant properties of a system based on temporally discretised realisations of individual trajectories. Thanks in particular to higher performance computing and storage in recent years, the technique has found its way into numerous fields of research [14, 15, 16, 17, 18]. Numerous conceptual approaches have been proposed to interpret these phase space trajectories. However, in this paper, recurrence plots as suggested by Eckmann *et al.* [19] and their quantification analysis (RQA) as further developed by Zbilut and Webber [20], then by Marwan et al. [21] are considered[1]. Section 2 will provide a detailed review of NTSA and RQA.

In this paper, a signal processing approach that uses RQA to enhance the detection of MLOs within sonar time series is proposed. Inspired by the study of femoral bone impaction in biomechanics [22], this initial study will demonstrate, through statistical analysis that several RQA measures are sufficient to significantly differentiate simulated sonar time series, developed based on work in [23], that contain buried target scatter from those that do not. While this study provides an early proof of concept, it is believed that by using RQA measures, additional insightful features of MLOs can be extracted from sonar time series. Such features could include the MLO material type or thickness and may remove the reliance on vast, detailed MLO databases, thereby making the processing robust to potential variability in the MLO scattering signature.

2. Nonlinear time series analysis

The nonlinear time series analyses presented in this paper are based on the theory of *dynamical systems*; that is, the time evolution of a system is defined in some phase space [12]. In the multidimensional phase space, all possible states of a system are represented along phase space trajectories, with each possible state corresponding to a unique point along the trajectory. Using the phase space, one can quantify certain dynamically invariant properties of a system based on temporally discretised realisations of individual trajectories [12]. In reality, as is the case in this paper, measurement data are limited to a finite number of scalar points in a time series; the phase space must therefore be reconstructed from the

---

[1]A comprehensive bibliography of RPs with theory and applications can be found here http://www.recurrence-plot.tk/bibliography.php

available *discrete* time series. State vectors can be reconstructed from scalar measurements by means of the delay embedding technique [12, 13, 21]. Delay embedding essentially rearranges a scalar time series, e.g., $x(t_n)$, into m-variate delay vectors, which can be defined through $x(t_n)$ as

$$\mathbf{x}(t_n) = [x(t_n), x(t_n + \tau), ..., x(t_n + (m-1)\tau)], \tag{1}$$

where τ and m are the time delay and embedding dimension, respectively. These are calculated (in this study) using the first minimum of the auto-mutual information and the false nearest neighbour of the time series, respectively [12].

2.1 Recurrence plots

The work in this paper focuses extracting useful information from phase space trajectories by utilising the concept of recurrences. The recurrent states of the trajectory $\mathbf{x}_i$ can be represented graphically by the binary recurrence matrix [21]

$$\mathbf{R}_{i,j}(\varepsilon) = \Theta(\varepsilon - ||\mathbf{x}_i - \mathbf{x}_j||), \quad i, j = 1, ..., N, \tag{2}$$

where N is the number of measured points, ε is a threshold distance which defines the size of the neighbour a trajectory must revisit to be considered recurrent, and $\Theta(\cdot)$ is the Heaviside function (i.e. $\Theta(x) = 0$, if $x < 0$, and $\Theta(x) = 1$ otherwise). Thus for states that recur within an ε-neighbourhood, the recurrence matrix is defined as

$$\mathbf{R}_{i,j} = \begin{cases} 1 : \mathbf{x}_i \approx \mathbf{x}_j, \\ 0 : \mathbf{x}_i \not\approx \mathbf{x}_j, \end{cases} \quad i, j = 1, ..., N. \tag{3}$$

In this study, the neighbourhood is defined using the fixed amount of neighbours (FAN) [15, 21].

2.2 Recurrence quantification

From the topological features of recurrence plots a variety of quantitative measures which relate to characteristics of the system can be extracted. This conceptual framework is known as recurrence quantification analysis (RQA) and has been widely used for real-time, time series analysis [24]. Several recurrence quantities have been highlighted as potentially useful for the detection of MLOs. In the following, similar to [22] where embedding parameters have been analysed, an approach that carries out statistical analyses using six recurrence quantities will be explored for the detection of MLOs in a range of simulated sonar time series. Table 1 lists the six recurrence quantities that will be used in this paper and provides a short description of what each represents in relation to the recurrence plots and the phase space.

3. Simulation based study

The acoustic scattering from five scenarios is evaluated using a finite element model. Each scenario represents a simplified potential underwater environment that MCM operations might encounter, i.e., empty seabed (no MLO), MLO sitting proud on the sea floor or MLO at some level of burial within the seabed. Figure 1 shows a cross-sectional schematic of the five scenarios investigated in this paper. From multistatic sonar scatter evaluated using these models, the six recurrence quantities defined in Table 1 are calculated and a statistical analysis is carried out to determine whether significant differences exist between the five datasets.

Table 1: List of six RQAs with a short description of what each represents in relation to recurrence plots and phase space.

Variable	Description
Determinism (DET)	Relates to the percentage of recurrence points that form diagonal lines (non-tangential motion)
	Measures predictability
Entropy ($ENTR$)	Entropy of the diagonal line length
	Decreases as the number of diagonals does
Laminarity (LAM)	States which remain fairly constant
	Relates to vertical lines (tangential motion)
Mean line length ($<L>$)	Relates to the average diagonal line length
	Decreases as a result of shorter average periods
Max line length (L_{max})	Maximal diagonal line length
Max vertical line length (V_{max})	Maximal vertical line length

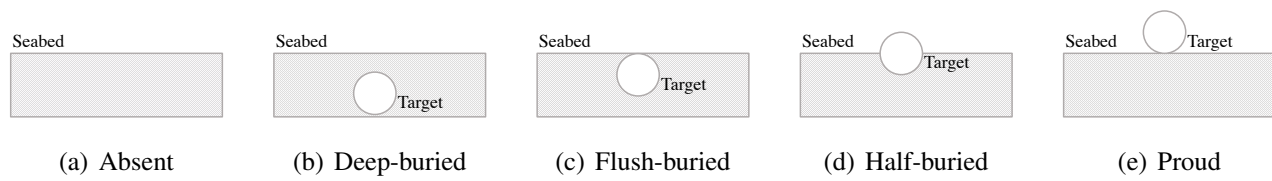(a) Absent   (b) Deep-buried   (c) Flush-buried   (d) Half-buried   (e) Proud

Figure 1: Cross-sectional schematics depicting the five simulated scenarios used to generate sonar time series for the analysis.

3.1 Simulation setup

Earlier work produced analytically validated FE models for spherical shells scattering within different fluid media [23]. In the work described here, these were developed further for a spherical stainless steel shell of radius 50 mm and thickness 0.55 mm using full-wave simulations in COMSOL Multiphysics. The interface between the seawater and the seabed has been modelled, with the shells positioned either side of, or embedded within, the seawater-seabed interface, according to the five scenarios in Fig. 1. The seawater and seabed domains were modelled using the Pressure Acoustics and Poroelastic Waves modules, respectively. The Solid Mechanics module was used to model the structural response of the shells. To enforce the Sommerfeld radiation condition, perfectly matched layers (PMLs) surrounded both domains. All scenarios modelled were axially symmetric, enabling three-dimensional solutions to be approximated with the reduced computational cost of performing two-dimensional, axisymmetric simulations. Figure 2 shows a schematic of the modelled geometry for a shell positioned just beneath the seawater-seabed interface, i.e. flush-buried case.

The modelling was implemented in the frequency domain with the outbound (i.e. to the target) sonar taking the form of a plane wave normal to the seabed. The pressure waves were chirped from 2 - 20 kHz in 20 Hz increments to propagate through the fluid domain with unit amplitude. The scattering spectra were evaluated at 46 evenly spaced positions along a half-circular arc 1 m from the surface interface. The scattering spectra were multiplied in the frequency domain by a model of the incident sonar pulse with the resulting products inverse Fourier transformed to obtain time series. A linear, 3 - 7 kHz swept
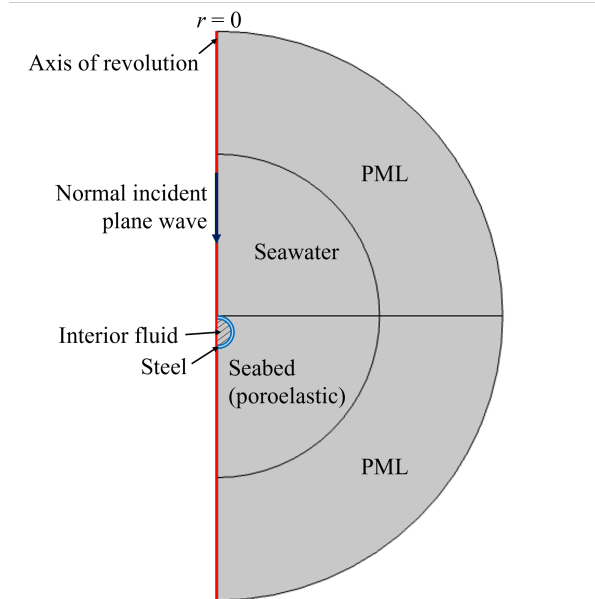
Figure 2: Schematic of half the spherical numerical model geometry.

cosine chirp, was used as the sonar pulse since the work in [23] indicated that this range excites strongly scattering target resonances whether proud or buried. The resulting time series signals were then matched filtered to enhance the scattered sonar returns that contain the target resonances. Figure 3 shows an example of the scattered pressure evaluated along the arc at $37.5°$ from the horizontal for the *absent* and *proud* scenarios. It can be observed that the introduction of the target results in a very subtle difference in the scattered pressure time series; differences become increasingly hard to notice as the target becomes further buried.
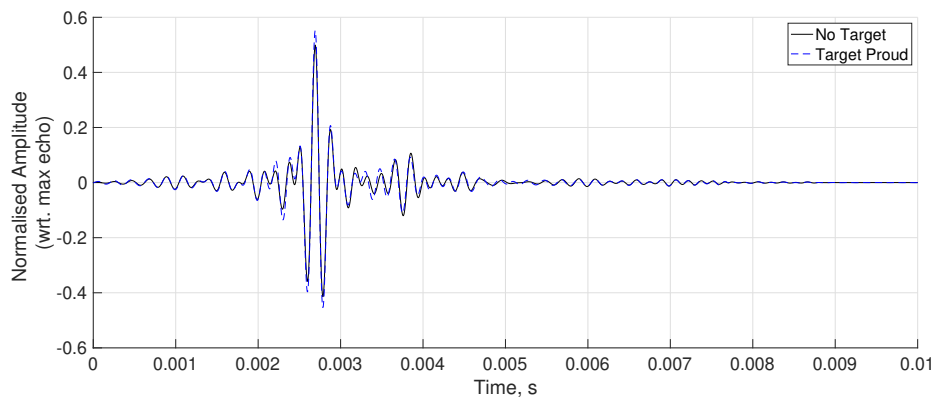

Figure 3: Scattered pressure evaluated for the model with no target vs. the model with proud target.

3.2 Statistical analysis using recurrence quantities

In this section, the results of statistical analyses, which use recurrence quantities to distinguish sonar returns containing target scatter from returns without, are presented. The six recurrence quantities listed in Table 1 have been calculated at each of the 46 evaluation points for all five of the scenarios shown in Fig

1. To establish if significant differences exist between the datasets, the recurrence quantities are grouped for each scenario and then analysed using one-way ANOVA tests [22]. These are then combined with a Tukeys test of significant difference *multi-compare* procedure, which was chosen as it is optimal for balanced one-way ANOVA tests with equal sample sizes, as is the case here. Figure 4 shows the results of the statistical analysis for each recurrence quantity. Each of the plots in Fig. 4 show the mean value of each recurrence quantity and their 95% confidence intervals, for each scenario. Two group means are significantly different if their intervals do not overlap; they are not significantly different if the intervals do overlap.
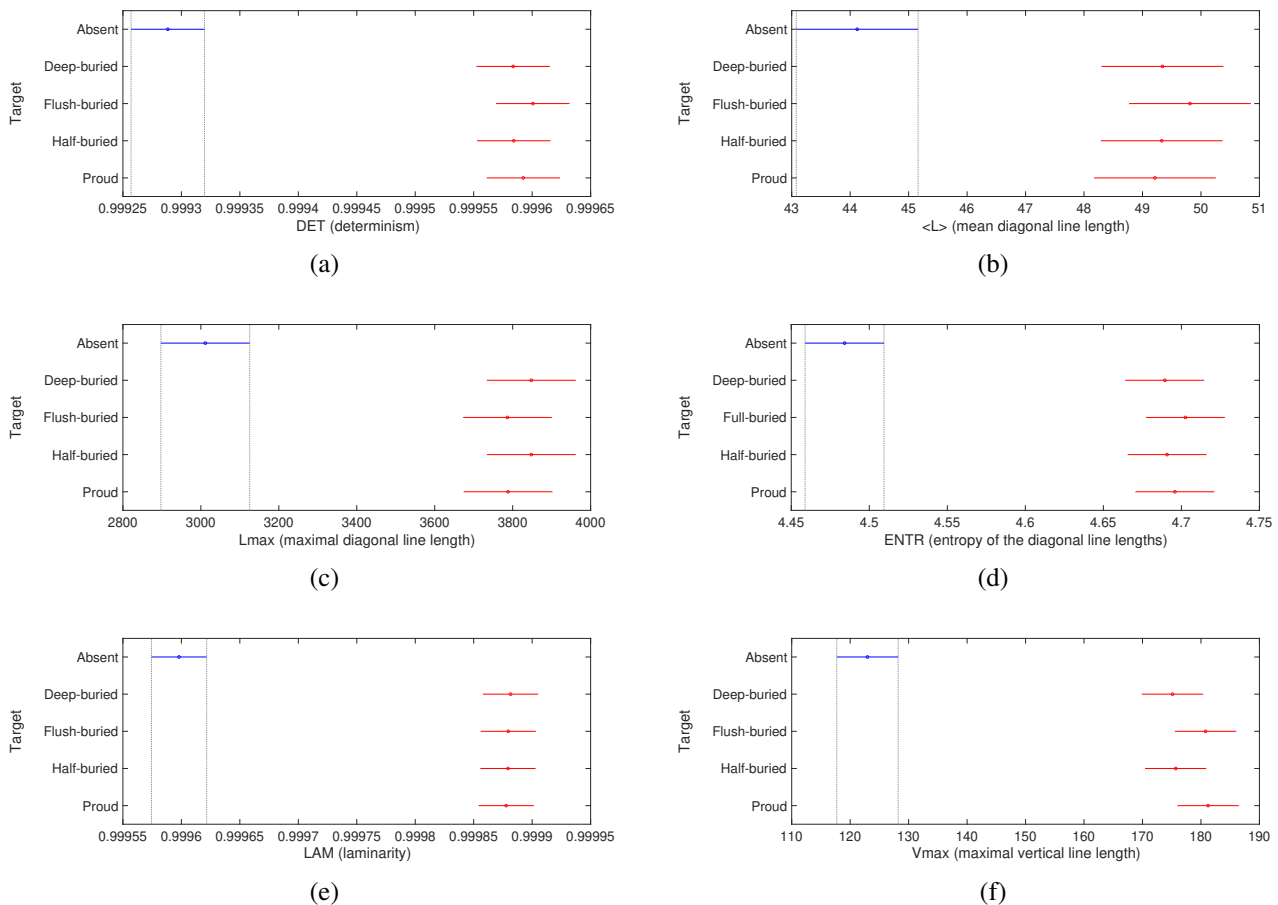

Figure 4: Results of the one way ANOVA tests for the recurrence quantities in each scenario. The group means are represented by a circle and the 95% confidence interval by a line extending out from the circle.

The results in Fig. 4 show that, for all six recurrence quantities, there is no overlap of the confidence intervals when a target is absent vs. when a target is present, irrespective of the level of burial. This indicates a significant difference between the mean values of these recurrence quantities. Further, in the simulations where a target is present, the mean value of the recurrence quantities cluster, showing no significant differences and indicating that there are commonalities in the time series which are picked up using RQA. This important finding demonstrates the potential for the use of RQAs in this way for the detection and classification of buried MLOs.

4. Conclusions

The concept of quantifying recurrence properties in phase space to characterise dynamical systems has recently attracted considerable interest and has been successfully applied to many real-world problems [16, 22]. The work in this paper has investigated the potential of using RQA to enhance the detection of buried and partially buried MLOs in sonar time series. The results showed that, using six recurrence quantities, there were significant differences between the mean values when a target is present, irrespective of the level of burial, vs. when the target is absent. Furthermore, no significant differences were found between the scenarios where a target was present, thereby indicating commonalities in the time series that may be exploited for target detection and classification. The next steps, which are currently ongoing, will be to investigate the robustness of the proposed MCM processing technique using both simulated and experimentally obtained datasets. Further work will look to utilise reconstructed recurrence quantity time series to enable classification of MLOs, i.e. to differentiate between targets with different properties in like scenarios.

Acknowledgements

REFERENCES

1. Bjørnø, L., *Applied Underwater Acoustics*, Elsevier, UltraTech Holding, Taastrup, Denmark (2017).

2. Council, N. R., *Naval Mine Warfare: Operational and Technical Challenges for Naval Forces*, The National Academic Press, Washington DC (2001).

3. Jans, W., Sternlicht, D. D., Williams, K. and Richardson, M. Emerging technologies in underwater munitions mapping, *4th Underwater Acoustics Conference and Exhibition*, pp. 669 – 676, (2017).

4. Langner, F., Knauer, C., Jans, W. and Ebert, A. Side scan sonar image resolution and automatic object detection, classification and identification, *OCEANS 2009-EUROPE*, pp. 1–8, (2009).

5. Thanh Le, H., Phung, S. L., Chapple, P. B., Bouzerdoum, A., Ritz, C. H. and Tran, L. C. Deep gabor neural network for automatic detection of mine-like objects in sonar imagery, *IEEE Access*, **8**, 94126–94139, (2020).

6. Baum, C. E. Discrimination of buried targets via the singularity expansion, *Inverse Problems*, **13**, 557 – 570, (1997).

7. Tesei, A., Fox, W. L. J., Maguer, A. and Løvik, A. Target parameter estimation using resonance scattering analysis applied to air-filled, cylindrical shells in water, *Journal of the Acoustical Society of America*, **108**, 2891 – 2900, (2000).

8. Tesei, A., Maguer, A., Fox, W. L. J., Lim, R. and Schmidt, H. Measurements and modeling of acoustic scattering from partially and completely buried spherical shells, *Journal of the Acoustical Society of America*, **112** (5), 1817 – 1830, (2002).

9. Maguer, A., Fox, W., Schmidt, H., Pouliquen, E. and Bovio, E. Mechanisms for subcritical penetration into a sandy bottom: Experimental and modelling results, *Journal of the Acoustical Society of America*, **107**, 1215 – 1225, (2000).

10. Lim, R. Naval Surface Warfare Center Panama City Division, Sonar detection and classification of underwater uxo and environmental parameters, (2012).

11. Oberst, S., Marburg, S. and Hoffmann, N. Determining periodic orbits via nonlinear filtering and recurrence spectra in the presence of noise, *Procedia Engineering*, **199**, 772–777, x International Conference on Structural Dynamics, EURODYN 2017, (2017).

12. Kantz, H. and Schreiber, T., *Nonlinear Time Series Analysis*, Cambridge University Press (2003).

13. Goswami, B. A brief introduction to nonlinear time series analysis and recurrence plots, *Vibration*, **2** (4), 332–368, (2019).

14. Acharya, U. R., Faust, O., Ghista, D. N., Sree, S. V., Alvin, A. P. C., Chattopadhyay, S., Lim, T.-C., Ng, E. Y.-K. and Yu, W. A systems approach to cardiac health diagnosis, *Journal of Medical Imaging and Health Informatics,*, **3** (2), 261 – 267, (2013).

15. Oberst, S., Niven, R. K., Lester, D. R., Ord, A., Hobbs, B. and Hoffmann, N. Detection of unstable periodic orbits in mineralising geological systems, *Chaos: An Interdisciplinary Journal of Nonlinear Science*, **28** (8), 085711, (2018).

16. Stender, M., Oberst, S., Tiedemann, M. and Hoffmann, N. Complex machine dynamics: systematic recurrence quantification analysis of disk brake vibration data, *Nonlinear Dynamics*, **97** (4), 2483–2497, (2019).

17. Banerjee, A., Goswami, B., Hirata, Y., Eroglu, D., Merz, B., Kurths, J. and Marwan, N. Recurrence analysis of extreme event-like data, *Nonlinear Processes in Geophysics*, **28** (2), 213–229, (2021).

18. Abid, M. and Lefebvre, G. Improving indoor geomagnetic field fingerprinting using recurrence plot-based convolutional neural networks, *Journal of Location Based Services*, **15** (1), 61–87, (2021).

19. Eckmann, J. P., Oliffson Kamphorst, S. and Ruelle, D. Recurrence plots of dynamical systems, *Europhysics Letters*, **4** (9), 973 – 977, (1987).

20. Zbilut, J. P. and Webber, C. L. Embeddings and delays as derived from quantification of recurrence plots, *Physics Letters A*, **171** (3), 199–203, (1992).

21. Marwan, N., Romano, M. C., Thiel, M. and Kurths, J. Recurrence plots for the analysis of complex structures, *Physics Reports*, **438**, 237 – 329, (2007).

22. Oberst, S., Baetz, J., Campbell, G., Lampe, F., Lai, J. C., Hoffmann, N. and Morlock, M. Vibro-acoustic and nonlinear analysis of cadavric femoral bone impaction in cavity preparations, *International Journal of Mechanical Sciences*, **144**, 739–745, (2018).

23. Milton, J., Hall, M., Chiang, Y. K., Halkon, B., Oberst, S. and Powell, D. Exploring the effect of underwater burial on the resonant behaviour of simplified shell geometries, *Accepted: In the Proceedings of the Australian Acoustical Society conference*, (2022).

24. Donner, R. V., Zou, Y., Donges, J. F., Marwan, N. and Kurths, J. Recurrence networks - a novel paradigm for nonlinear time series analysis, *New Journal of Physics*, **12** (033025), (2010).